Electronic supplementary information (ESI)

The role of viscosity in various dynamical processes of different fluorophores in ionic liquid–cosolvent mixtures: a femtosecond fluorescence upconversion study

Rupam Dutta,[a] Gourhari Jana,[b] Dipankar Mondal,[a] Arghajit Pyne,[a] Sourav Sil,[a]‡ Pratim K. Chattaraj*[b] and Nilmoni Sarkar *[a]

[a]Department of Chemistry, Indian Institute of Technology Kharagpur, Kharagpur,721302 WB, India. E-mail: nilmoni@chem.iitkgp.ac.in, nilmonisarkar1208@gmail.com;
Fax: +91-3222-255303
[b]Department of Chemistry and Center for Theoretical Studies, Indian Institute of Technology Kharagpur, Kharagpur, 721302 WB, India.
E-mail: pkc@chem.iitkgp.ac.in

‡Present address: Department of Chemistry, Michigan State University, East Lansing, Michigan 48824-1322, USA.

Contents

1. Instrumentation

1.1. Viscosity (η) measurements

The bulk viscosities of different room temperature ionic liquid (RTIL)-cosolvent mixtures are measured using a Brookfield DV-II+ Pro viscometer at 298 K. 1 mL of each of the solutions are used for the determination of bulk viscosities at different rpm values and the average values have been calculated.

1.2. Steady state absorption and emission measurements

The steady state absorption spectra of C153 different room temperature ionic liquid (RTIL)-cosolvent mixtures are recorded by Shimadzu (model no UV-2450) spectrophotometer. Simultaneously, the emission spectra of the same solution are measured using Hitachi (model no. F-7000) spectrofluorimeter. To collect the emission spectra C153 samples are excited at 400 nm.

1.3. Femtosecond fluorescence upconversion measurements

Femtosecond fluorescence traces are taken in our femtosecond fluorescence upconversion set up where the excitation source is solid state Ti-sapphire laser (Mai Tai HP, Spectra-Physics) with a tunable range from 690 nm to 1040 nm. In our experiment, we have used ~100 fs pulse centered at 800 nm with a repetition rate of 80 MHz. Our experimental set up is commercially available from IB photonics, model Fluomax-SC (Bulgaria). In this set up fundamental 800 nm beam is focused onto a thin β-barium Borate (BBO) crystal which generates a frequency doubled visible pump beam centered at 400 nm. The remaining fundamental, which acts as gate beam and frequency doubled 400 nm, is separated through a dichroic mirror. The fluorescence is collected from the sample and focused on another thin BBO crystal for the type I frequency upconversion with the fundamental gate pulse. The gate pulse is time delayed with respect to the fluorescence using computer controlled motorized optical delay line. The upconverted signal is focused on the entrance slit of a double

monochromator and detected by a photomultiplier tube (Hamamatsu). All the emission decays are collected in magic angle (54.7°) polarization. Throughout the experiment, we have used ~10 mW power of pump laser to excite the sample, taken in a rotating sample holder. Our instrument response function (IRF) is estimated around ~250 fs. The femtosecond fluorescence kinetics are taken at the respective emission maxima and deconvoluted using a Gaussian-shaped IRF by Labview software using a multi-exponential function, $I(\lambda,t)=\sum_i a_i(\lambda,t)exp(-t/\tau_i(\lambda))$ where $a_i(\lambda)$ is the contribution of corresponding $\tau_i(\lambda)$ decay times.

1.4. Time resolved anisotropy measurements

The time-resolved anisotropy decays were recorded using time correlated single photon counting (TCSPC) instrument from IBH (U.K.) In TCSPC set up, a picosecond diode laser (IBH, Nanoled) of 402 nm was used as excitation source. During anisotropy measurement, a motorized polarizer was used on the emission side using a Hamamatsu microchannel plate photomultiplier tube (3809U). The emission decays were collected at parallel $I_{\parallel}(t)$ and perpendicular $I_{\perp}(t)$ polarizations at regular time intervals until the desired peak difference between $I_{\parallel}(t)$ and $I_{\perp}(t)$emission decays was reached. The following equation was used to calculate the time-resolved anisotropy ($r(t)$) [75,76]

$$r(t)=\frac{I_{\parallel}(t)-GI_{\perp}(t)}{I_{\parallel}(t)+2GI_{\perp}(t)} \quad (1)$$

The correction factor, G, has been calculated using horizontally polarized excitation light. The horizontal ($I_{\parallel}$) and vertical ($I_{\perp}$) components of the emission decay were collected through the emission monochromator when the emission polarizer was fixed at horizontal and vertical positions, respectively. In our TCSPC setup, G value was 0.6. During the analysis of time-resolved decays, we have used IBH DAS-6 decay analysis software.

1.5. Fluorescence correlation spectroscopy (FCS) measurements

FCS correlates the fluorescence fluctuations which originate from the variation in the concentration of the fluorescent species due to the translational motion or the chemical reaction or complex formation into or out of the confocal volume (~1 femtolitre).

The correlation function, $G(\tau)$ which is used to describe the temporal fluctuation of fluorescence intensity is defined as

$$G(\tau)=\frac{\langle\delta F(t)\delta F(t+\tau)\rangle}{\langle F(t)\rangle^2} \quad (2)$$

Where $\delta F(t)$ represents the fluctuation of fluorescence signal $F(t)$ as deviations from the temporal average of the signal $\langle F \rangle$ at time t. Therefore, $\delta F(t) = F(t) - \langle F \rangle$.

FCS traces of 4-(dicyanomethylene)-2-methyl-6-(*p*-dimethylaminostyryl)-4*H*-pyran (DCM) in different room temperature ionic liquid (RTIL)-cosolvent mixtures are carried out using DCS 120 Confocal Laser Scanning Microscope (CLSM) system (Becker &Hickl DCS-120) with inverted optical microscope of Zeiss (Carl Zeiss, Germany) and it is equipped with a 40X water immersion objective (Numerical Aperture =1.2). A very low concentration of dye solution (~1 nM) is placed on glass cover slip and excited at 488 nm from a picosecond diode laser (bh BDL-SMC). The laser is operated in the CW mode. Scanning of the sample is controlled by bh GVD-120 scan controller. A main dichroic filter is used to separate the fluorescence signal from the excitation light. The fluorescence signal is then split into two channels after focusing onto a 50/50 beam splitter through a pinhole and finally collected by two single photon avalanche diodes (SPADs) connected with two channels. A correlator card is used to record the fluorescence autocorrelation traces from the signals of two detectors. For room temperature ionic liquid (RTIL)-cosolvent mixtures a bi-component diffusion equation is used in order to fit the autocorrelation functions

$$G(\tau) = \frac{1}{N}\left[1 + \frac{\tau}{\tau_D}\right]^{-1}\left[1 + \frac{\tau}{S^2\tau_D}\right]^{-\frac{1}{2}} \quad (3)$$

In this equation, *N* is the average number of fluorescent molecules in the detection volume, and τ_D is the average time of fluorescent molecules diffusing in the detection volume with their corresponding amplitude (A). *S* is the structure parameter which is equal to the $\frac{\omega_z}{\omega_{xy}}$ where ω_z is the longitudinal radius and ω_{xy} is the transversal or waist radius of the confocal volume. τ_D is related to the translational diffusion coefficient (D_t) by the following equation

$$\tau_D = \frac{{\omega_{xy}}^2}{4Dt} \quad (4)$$

The structure parameter (*S*) of the excitation volume is determined using DCM in water as a reference sample of known diffusion coefficient (D_t = 310 $\mu m^2 s^{-1}$). The value of structure parameter is found to be 5. This value has been fixed for the analysis of all data obtained in our systems. Fitting of the FCS data of DCM in water shows the diffusion time of ~107 μs which has been used to calculate the transverse radius and the confocal volume of our set-up. The calculated transverse radius is ~365 nm and the confocal volume is 1.35 *f*L.

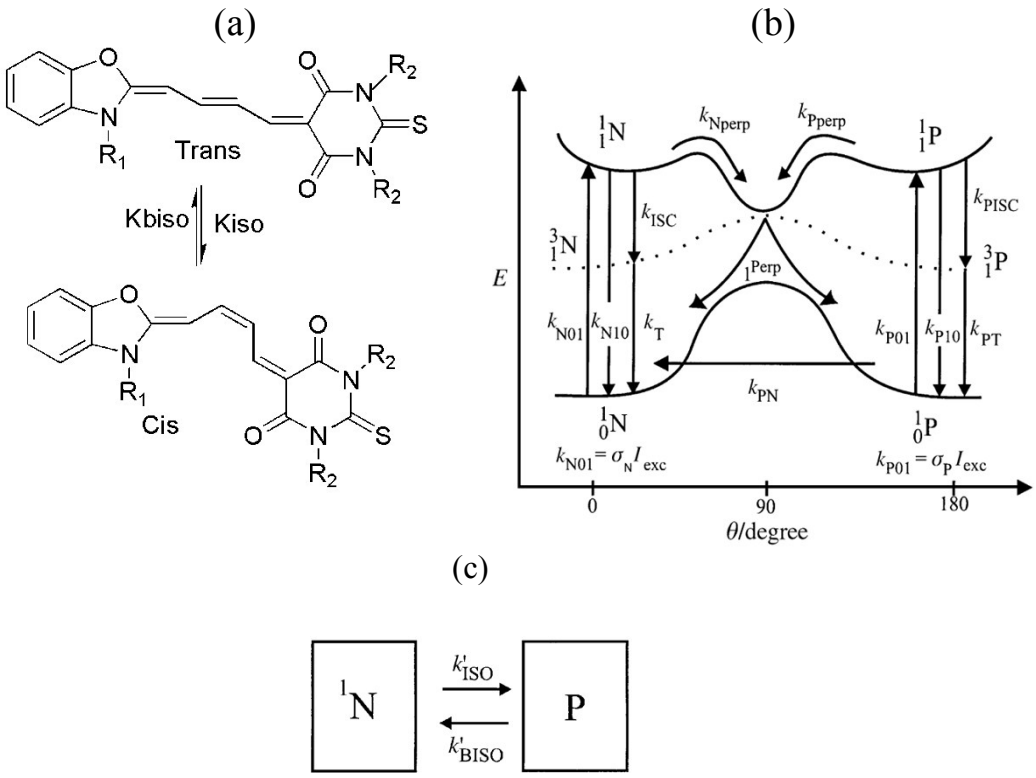

Scheme S1. (a) Chemical structure and photoisomerization of cyanine dyes (b) generalized model used for photoisomerization of cyanine dyes (c) simplified photophysical model for cyanine dyes (k_{iso}*is defiend as the rate of isomerization from trans state to cis state*)

In scheme S1(b), the horizontal direction corresponds to the torsional angle around the double bond of the polymethylene chain of MC-540 (denoted as θ) and the vertical direction corresponds to the energy. The ${}^1_0N$, ${}^1_1N$, ${}^3_1N$ denote the ground singlet, excited singlet and triplet state of all trans forms. k_{N01} and k_{N10} are the rate of excitation from ${}^1_0N$ state to ${}^1_1N$ state and rate of deactivation from ${}^1_1N$ to ${}^1_0N$ state. k_{ISC} and k_T denotes the deactivation to triplet state and ground state respectively. ${}^1_1Perp$ is the intermediary twisted excited state at half rotational angle. It is formed form ${}^1_1N$ or ${}^1_1P$ state with the rate constant of k_{NPerp} or k_{PPerp} and then, it is further deactivated to ${}^1_0N$ or ${}^1_0P$ state in picosecond to nanosecond time scale. Molecules can also relax from ${}^1_0P$ state to ${}^1_0N$state in millisecond time scale. Moreover, the cis isomers are non-fluorescent in nature. Thus, the fluorescence brightness of cis isomer can be neglected due to very fast deactivation channel through internal conversion. The

quantum yield from ${}^1_1P$ is very low and consequently, the population of ${}^3_1P$ should be very small and will not be further taken into consideration.

Thus, considering these factors and disregarding any triplet state formation in these dyes, the photophysical model in (S1(b)) can be simplified into two state model (S1(c)) which contain fluorescent N form (${}^1_0N, {}^1_1N$) and non-fluorescent P form (${}^1_0P, {}^1_1P$). Under the condition which is relevant to this system, the electronic state of merocyanine-540 can be described by a two state model; fluorescent trans form (N) and non-fluorescent cis form (P),

$$N \rightleftharpoons P \tag{5}$$

If the fluorescence fluctuations arises from the translational diffusion and fluorescence blinking originating from transitions between a fluorescent trans isomer (*N*) and non-fluorescent cis isomer (*P*) as modeled in fig. (S1(c)), the correlation function can be defined by

$$G(\tau) = \frac{1}{N}\left(\frac{1}{1 + (\tau/\tau_D^i)}\right)\left(\frac{1}{1 + \frac{1}{\omega^2}(\frac{\tau}{\tau_D^i})}\right)^{1/2}\left(1 + \frac{P_{eq}}{1 - P_{eq}}\exp(-\tau/\tau_{iso})\right) \tag{6}$$

In the above equation, P_{eq} is the time and space averaged fraction of fluorophores within the detection volume being in a non-fluorescentcis photo isomer form and τ_{iso} is the relaxation time related to trans cis process. Now, if we approximate the excitation irradiation distribution within the detection volume is uniform, P_{eq} and τ_{iso} can be written as

$$P_{eq} = \frac{k_{ISO}^{/}}{k_{ISO}^{/} + k_{BISO}^{/}}$$

$$\tau_{ISO} = (k_{ISO}^{/} + k_{BISO}^{/})^{-1}$$

$$P_{eq} = k_{ISO}^{/}\tau_{ISO} \tag{7}$$

$K_{ISO}^{/}$and$K_{BISO}^{/}$can be related to K_{ISO} and $K_{BISO}$by the following equations,

$$K_{ISO}^{/} = \frac{\sigma_N I_{exc}}{\sigma_N I_{exc} + k_{N10}} k_{ISO}$$

$$K_{BISO}^{/} = \frac{\sigma_P I_{exc}}{\sigma_P I_{exc} + K_{P10}} k_{BISO} \approx \sigma_{BISO} I_{exc} \qquad (k_{P10} \gg \sigma_P I_{exc})$$

(8)

Where I_{exc} is the excitation energy, σ_N and σ_P are the excitation cross sections of N_0 and P_0 states and σ_{BISO} denotes the effective cross section for back isomerizaion of the cis state.

Table S1: Absorption maxima, emission maxima and viscosity of C153 in [EmimES] RTIL in presence of different cosolvents

System	Mole fraction of cosolvent	λ_{max}^{abs} (nm)	λ_{max}^{em} (nm)	Viscosity(cP)
Neat [EmimES]	-	431	533	61.56±0.2
Water in [EmimES]	0.5	433	540	18.21±0.3
	0.6	434	542	11.15±0.2
	0.7	435	543	8.75±0.3
	0.8	436	545	5.25±0.3
	0.9	437	546	3.42±0.2
MeOH in [EmimES]	0.5	432	535	22.35±0.2
	0.6	432	536	17.42±0.3
	0.7	432	536	11.84±0.2
	0.8	432	536	6.45±0.3
	0.9	432	536	2.85±0.2
iPrOH in [EmimES]	0.5	432	533	20.85±0.9
	0.6	432	533	17.54±0.8
	0.7	432	533	10.25±0.6
	0.8	432	533	7.47±0.3
	0.9	432	533	2.5±0.2

Table S2: Absorption maxima, emission maxima and viscosity of C153 in [EmimOS] RTIL presence of different cosolvents

System	Mole fraction of cosolvent	λ_{max}^{abs} (nm)	λ_{max}^{em} (nm)	Viscosity(cP)

Neat [EmimOS]	-	428	528	439.2±4.2
Water in [EmimOS]	0.5	430	532	97.4±2.8
	0.7	431	535	63±1.5
	0.9	432	539	22.4±1.4
MeOH in [EmimOS]	0.5	429	530	129.3±1.4
	0.7	429	531	77.5±1.5
	0.9	430	532	22±1.2
iPrOH in [EmimOS]	0.5	430	528	137.4±1.8
	0.7	430	528	65.7±1.4
	0.9	431	528	11.5±0.5

Table S3: Time-resolved anisotropy decay parameters of C153 on addition of different cosolvents in neat [EmimES]

System	**Mole fraction of cosolvent**	r_0	a_1	a_2	τ_1 **(ps)**	τ_2 **(ps)**	$<\tau_{rot}>$ **(ps)**
Water in [EmimES]	0.2	0.40	0.18	0.82	196±5	2524±25	2105
	0.4	0.40	0.15	0.85	112±5	1652±19	1421
	0.5	0.39	0.18	0.82	137±24	970±24	820
	0.6	0.39	0.24	0.76	233±15	915±15	751.1
	0.7	0.39	0.16	0.84	53±3	665±17	567.2
	0.8	0.38	0.16	0.84	51±5	428±12	367.7
	0.9	0.38	0.13	0.87	15±1	221±8	194.3
MeOH in [EmimES]	0.2	0.40	0.21	0.79	145±7	1986±12	1599
	0.4	0.40	0.20	0.80	123±5	1221±14	1001
	0.5	0.39	0.18	0.82	26±1	613±10	507.3
	0.6	0.39	0.15	0.85	27±2	326±6	281.2
	0.7	0.38	0.21	0.79	25±2	218±5	177.5
	0.8	0.38	0.18	0.82	9±0.6	122±5	101.6

	0.9	0.37	0.15	0.85	8±0.5	79±2	68.4
iPrOH in [EmimES]	0.2	0.40	0.24	0.76	138±10	2027±56	1574
	0.4	0.40	0.23	0.77	137±9	1285±48	1021
	0.5	0.32	0.23	0.77	41±3	461±18	364.4
	0.6	0.30	0.26	0.74	27±1.2	356±11	270.5
	0.7	0.28	0.27	0.73	22±1	247±7	186.2
	0.8	0.28	0.30	0.70	19±1.4	143±7	106
	0.9	0.28	0.22	0.78	12±1.5	88±7	71

Table S4: Decay parameters of $C(t)$ of C153 on addition of different cosolvents in neat [EmimES]

System	**Mole fraction of cosolvent**	a_1	a_2	τ_1 **(ps)**	τ_2 **(ps)**	$<\tau_s>$ **(ps)**	$\upsilon(0)\_\upsilon(\infty)$ **(cm^{-1})**	$\upsilon(\infty)$ **(cm^{-1})**
Water in [EmimES]	0.2	0.76	0.24	175±7	804±9	326	4428	17957
	0.4	0.77	0.23	147±8	603±8	252	4413	17996
	0.5	0.37	0.63	31±3	307±5	205	3208	18502
	0.6	0.48	0.52	26±2	256±4	145.6	3203	18507
	0.7	0.52	0.48	24±1.5	197±4	107.4	3194	18515
	0.8	0.60	0.40	16±1	105±5	51.6	3175	18532
	0.9	0.62	0.38	8±0.5	65±4	29.7	3162	18544
MeOH in [EmimES]	0.2	0.74	0.26	141±3	649±6	273	4461	17961
	0.4	0.82	0.18	123±5	554±6	201	4442	17993
	0.5	0.65	0.35	81±5	345±7	173.4	3205	18504
	0.6	0.65	0.35	66±5	254±7	131.8	3200	18509
	0.7	0.51	0.49	27±2	145±6	84.8	3186	18522

	0.8	0.45	0.55	6.4±0.4	79.5±7	46.6	3172	18535
	0.9	0.36	0.64	3.3±0.4	34.1±6	23.2	3159	18546
iPrOH in [EmimES]	0.2	0.71	0.29	135±4	635±3	280	4455	17953
	0.4	0.70	0.30	131±3	431±7	221	4452	17992
	0.5	0.68	0.32	93±3	356±5	177.2	3205	18504
	0.6	0.66	0.34	55±3	312±5	142.3	3202	18507
	0.7	0.63	0.37	52±2	225±5	116.1	3198	18510
	0.8	0.61	0.39	40±2	130±4	75.1	3188	18518
	0.9	0.62	0.38	8±0.4	44±4	21.7	3159	18545

Table S5: Decay parameters of *C*(*t*) of C153 on addition of water in neat [EmimES] and [EmimOS]

System	Mole fraction of cosolvent	a_1	a_2	a_3	τ_1 (ps)	τ_2 (ps)	τ_3 (ps)	$<\tau_s>$ (ps)
Water in [EmimES]	0.5	0.08	0.47	0.45	0.36±0.02	195±4	1377±24	711.33
	0.7	0.10	0.50	0.40	0.34±0.03	99±6	859±18	393.13
	0.9	0.12	0.50	0.38	0.31±0.02	60±2	225±11	115.54
Water in [EmimOS]	0.5	0.07	0.53	0.40	0.43±0.02	89±4	847±9	386
	0.7	0.08	0.64	0.28	0.41±0.03	38±3	569±5	183.7
	0.9	0.09	0.68	0.23	0.40±0.03	8±0.7	91±6	26.41

Table S6: Stretched exponential fitting parameters of *C*(*t*) of C153 on addition of different cosolvents in neat [EmimES]

System	Mole fraction	τ_0	β	$<\tau_{solv}>$	$\upsilon(0)$-$\upsilon(\infty)$	$\upsilon(\infty)$

	of cosolvent				(cm^{-1})	(cm^{-1})
Water in [EmimES]	0.5	155.1±4	0.75	184	3206	18501
	0.6	108.5±2.3	0.67	143.5	3200	18504
	0.7	86.95±2.5	0.69	111.6	3193	18515
	0.8	70.6±1.2	0.65	96.5	3175	18532
	0.9	63.66±1	0.69	81.7	3164	18542
MeOH in [EmimES]	0.5	125.5±3.5	0.71	156.8	3208	18505
	0.6	83.76±4	0.65	114.5	3203	18512
	0.7	47.4±2	0.61	69.8	3187	18520
	0.8	27.76±0.9	0.64	38.6	3170	18533
	0.9	12.1±0.5	0.62	17.5	3158	18544
iPrOH in [EmimES]	0.5	135±3	0.74	162.5	3205	18504
	0.6	109.9±3	0.76	129.3	3201	18508
	0.7	72.7±2	0.64	101.1	3199	18511
	0.8	44.70±2.2	0.65	61.1	3185	18516
	0.9	11.22±0.6	0.69	14.4	3158	18544

Table S7: Stretched exponential fitting parameters of of *C*(*t*) of C153 on addition of different cosolvents in neat [EmimOS]

System	Mole fraction of cosolvent	τ_0 (ps)	β	$<\tau_{solv}>$ (ps)	$\upsilon(0)\_\upsilon(\infty)$ (cm^{-1})	$\upsilon(\infty)$ (cm^{-1})
Water in [EmimOS]	0.5	564.9±11	0.68	735.7	3268	18445
	0.7	330.1±5	0.71	412.2	3243	18473
	0.9	77.9±3	0.62	112.5	3202	18508
MeOH in [EmimOS]	0.5	253.1±6	0.62	365.4	3235	18477
	0.7	25.6±2.2	0.65	175.4	3208	18501
	0.9	16.55±0.7	0.74	19.9	3164	18543
iPrOH in [EmimOS]	0.5	157.7±5.5	0.59	242.5	3214	18495
	0.7	86.4±2.2	0.63	122.5	3241	18470
	0.9	13.77±0.8	0.66	18.5	3161	18545

Table S8: Diffusion coefficients (D_t) of DCM on addition of different cosolvents in neat [EmimES]

System	Mole fraction of cosolvent	a_1	a_2	D_{t1} ($\mu m^2 s^{-1}$)	D_{t2} ($\mu m^2 s^{-1}$)
Water in [EmimES]	0.5	0.72	0.28	101±4	34±3
	0.7	0.75	0.25	121±5	37±3
	0.9	0.78	0.22	278±10	41±5
MeOH in [EmimES]	0.5	0.74	0.26	161±5	48±2
	0.7	0.79	0.21	175±5	56±2
	0.9	0.88	0.12	284±9	72±4
iPrOH in [EmimES]	0.5	0.75	0.25	165±5	61±3
	0.7	0.80	0.20	186±4	68±4
	0.9	0.87	0.13	287±10	74±4

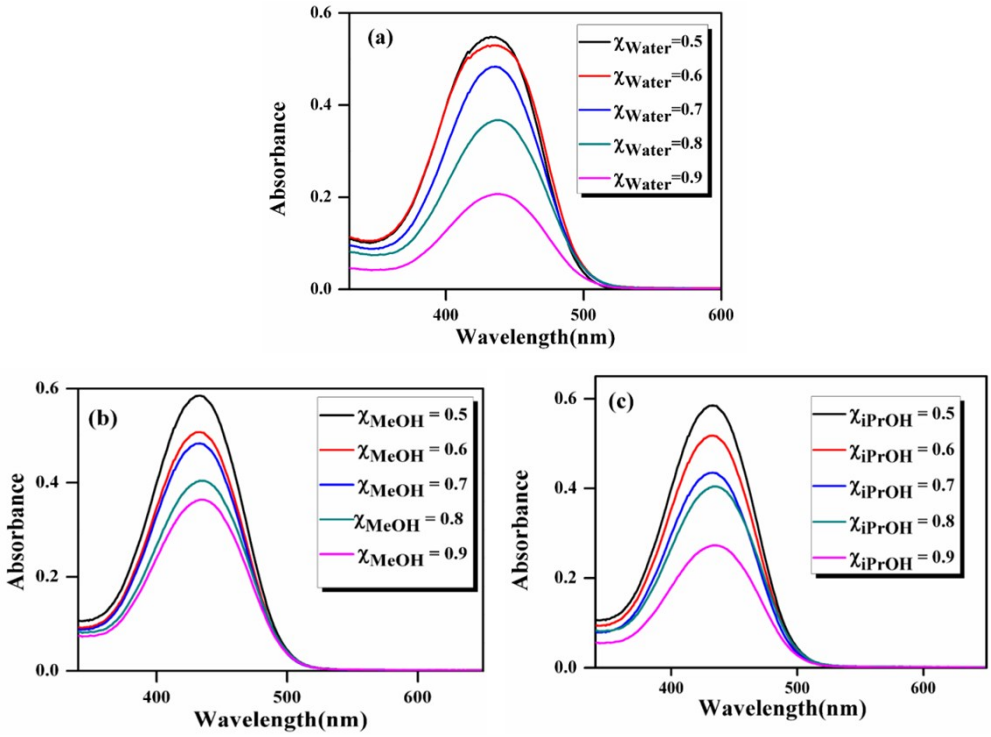

Fig. S1: Absorption spectra of C153 on addition of different cosolvents (a) water (b) MeOH (c) iPrOH in neat [EmimES].

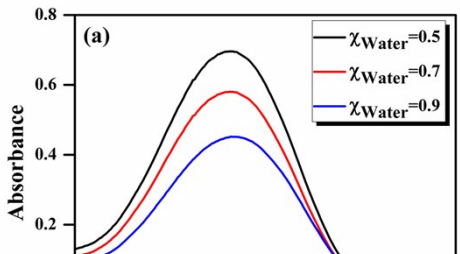

Fig. S2: Absorption spectra of C153 on addition of different cosolvents (a) water (b) MeOH (c) iPrOH in neat [EmimOS].

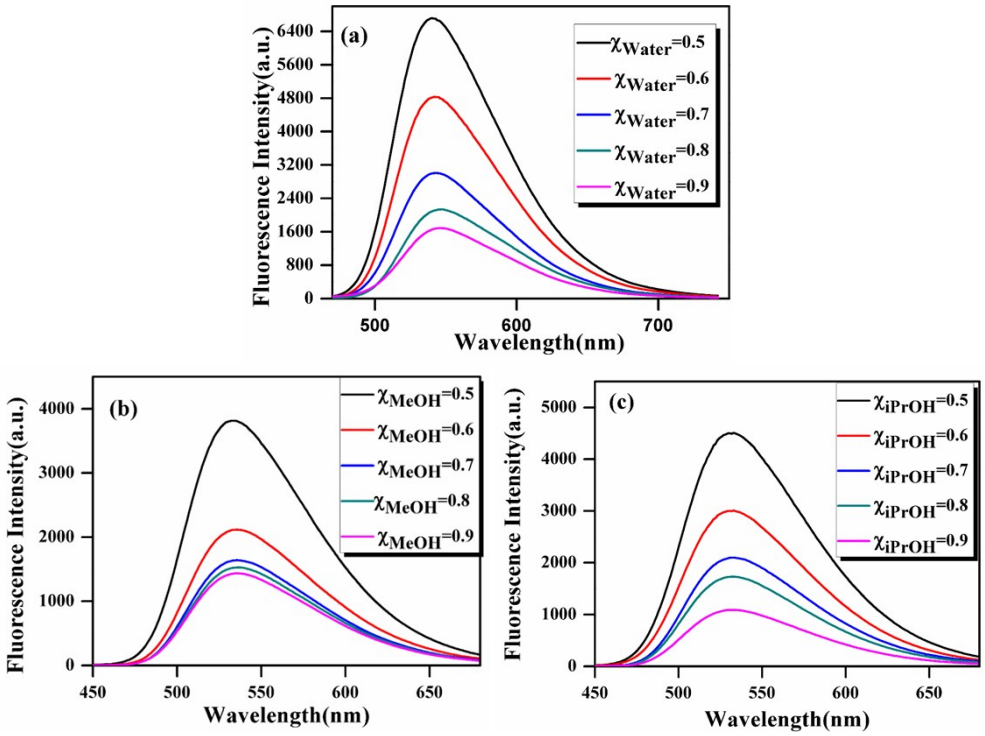

Fig. S3: Emission spectra of C153 on addition of different cosolvents (a) water (b) MeOH (c) iPrOH in neat [EmimES].

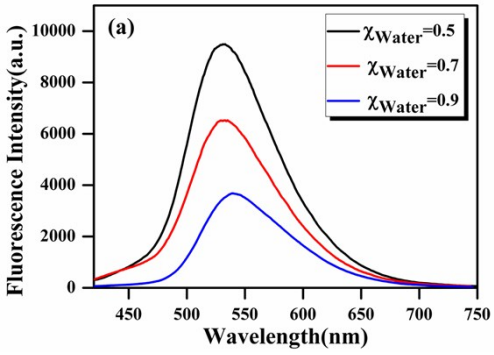

Fig. S4: Emission spectra of C153 on addition of different cosolvents (a) water (b) MeOH (c) iPrOH in neat [EmimOS].

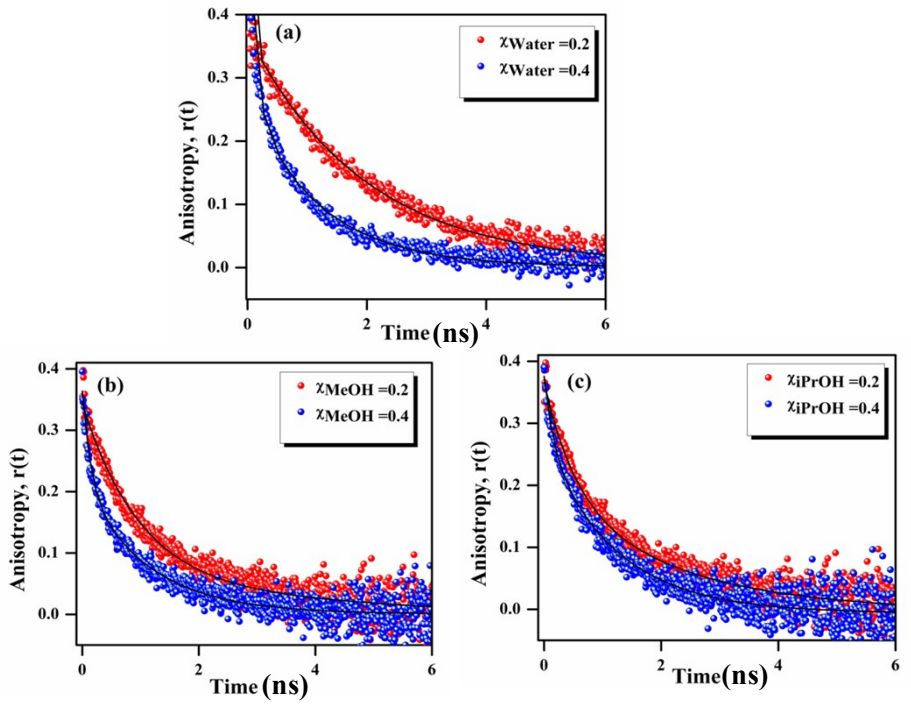

Fig. S5: Fluorescence anisotropy decays [r(t)] of C153 (λ_{ex}=402 nm) on addition of different cosolvents at low mole fractions (a) water (b) MeOH (c) iPrOH in neat [EmimEs].

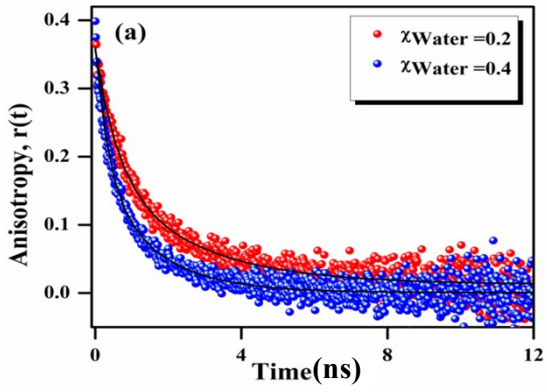

Fig. S6: Fluorescence anisotropy decays [r(t)] of C153 (λ_{ex}=402 nm) on addition of different cosolvents at low mole fractions (a) water (b) MeOH (c) iPrOH in neat [EmimOs].

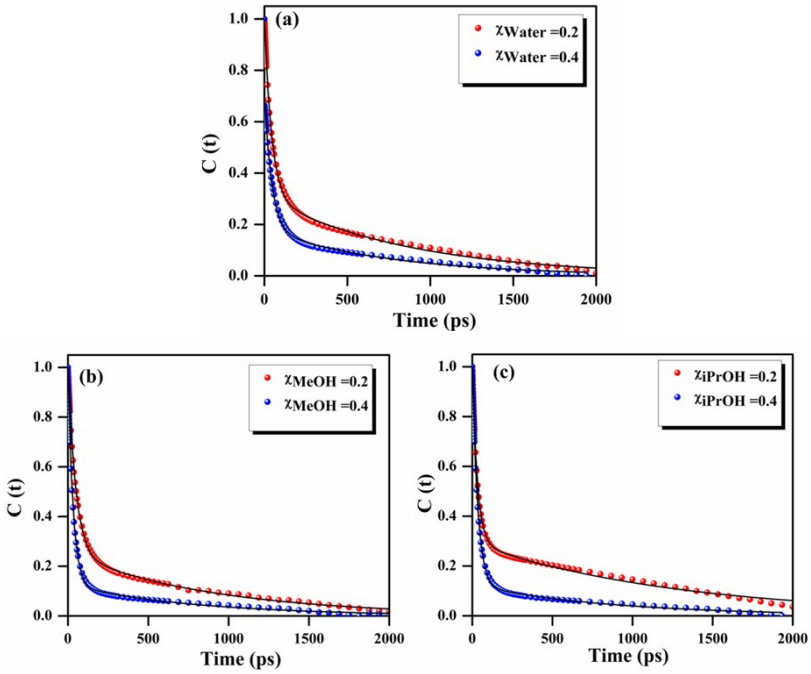

Fig. S7: Decay plots of solvent correlation function, ($C(t)$) of C153 (λ_{ex}=402 nm) on addition of different cosolvents at low mole fractions (a) water (b) MeOH (c) iPrOH in neat [EmimEs].

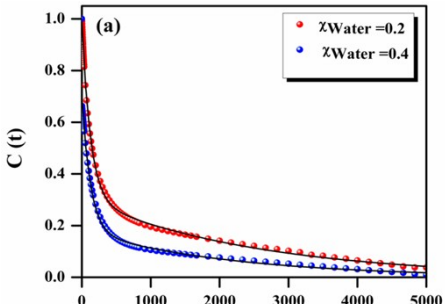

Fig. S8: Decay plots of solvent correlation function, ($C(t)$) of C153 (λ_{ex}=402 nm) on addition of different cosolvents at low mole fractions (a) water (b) MeOH (c) iPrOH in neat [EmimOs].

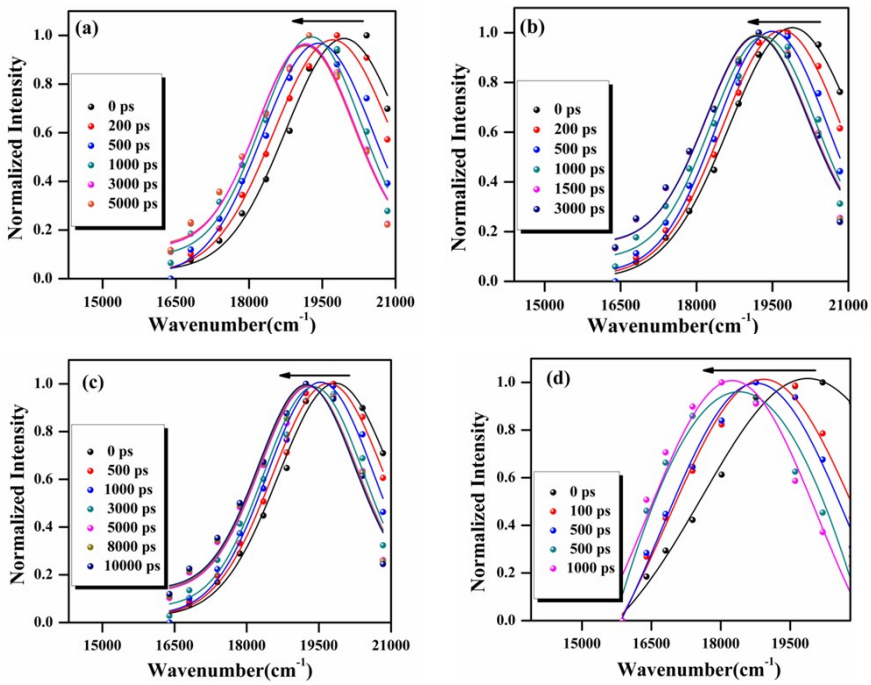

Fig. S9: Time-resolved emission spectra (TRES) of C153 in (a) 0.5 mole fraction of water in [EmimEs]-water mixture, (b) 0.9 mole fraction of iPrOH in [EmimEs]-water mixture, (c) 0.5 mole fraction of water in [EmimOs]-water mixture, (d) 0.9 mole fraction of iPrOH in [EmimOs]-water mixture.

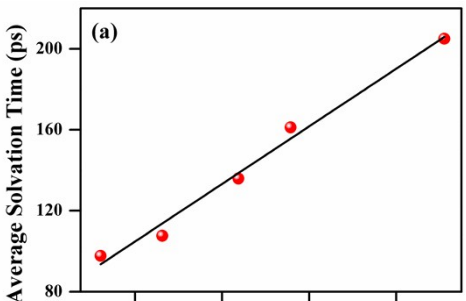

Fig. S10: Plot of average solvation time of C153 vs bulk viscosity in presence of different cosolvents (a) water (b) MeOH (c) iPrOH in neat [EmimES].

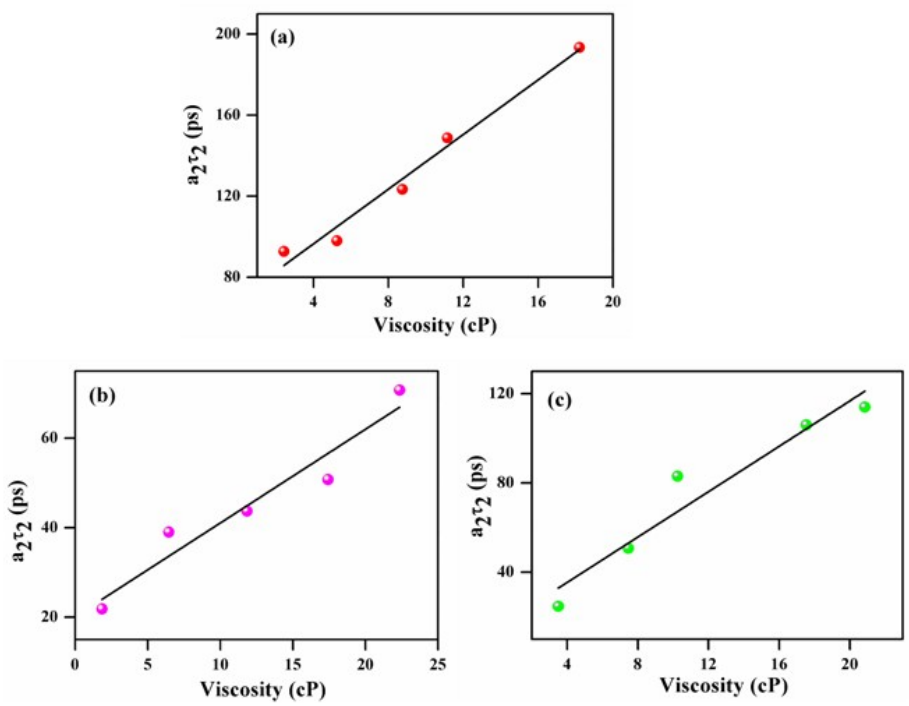

Fig. S11: Plot of $a_2\tau_2$ of C153 vs bulk viscosity in presence of different cosolvents (a) water (b) MeOH (c) iPrOH in neat [EmimES].

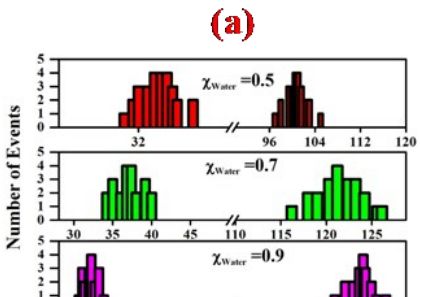

Fig. S12: Distribution of D_t values obtained by performing the FCS experiments more than 10 times.

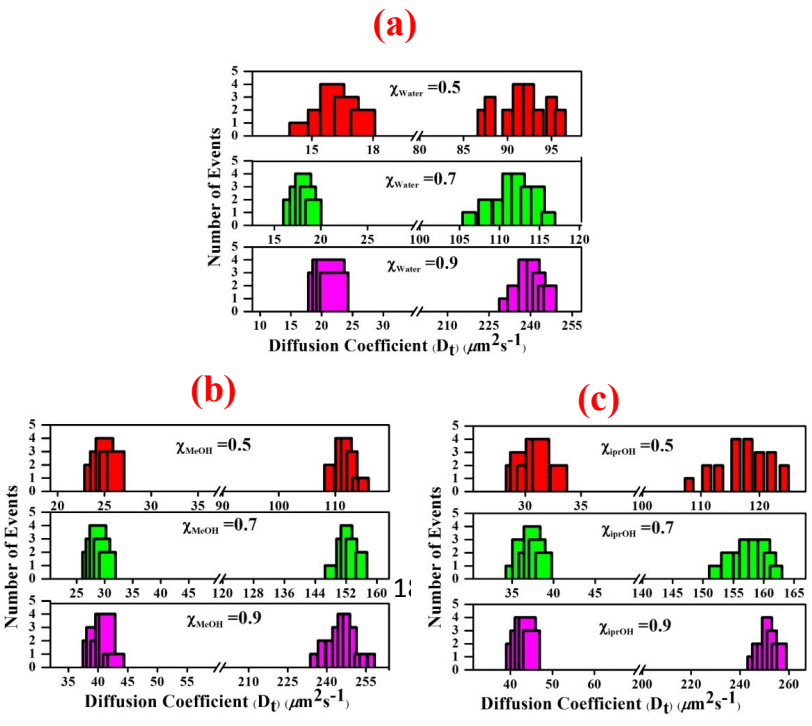

Fig. S13: Distribution of D_t values obtained by performing the FCS experiments more than 10 times.

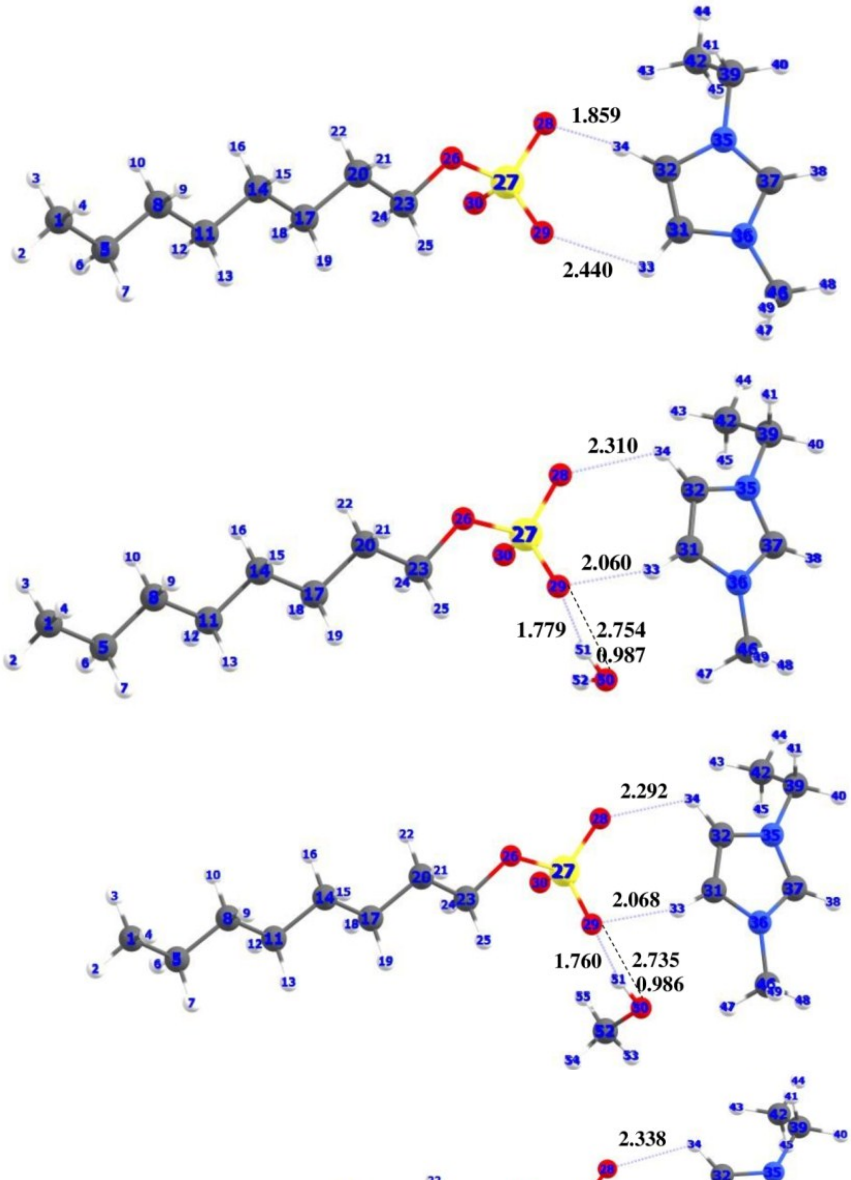

Fig. S14a: Optimized geometries of the [EmimOs], [EmimOs]-water, [EmimOs]-MeOH, [EmimOs]-iPrOH complexes, calculated at the B3LYP/6-31++G(d,p) level in the gas phase. Bond distances are given in Angstrom unit.

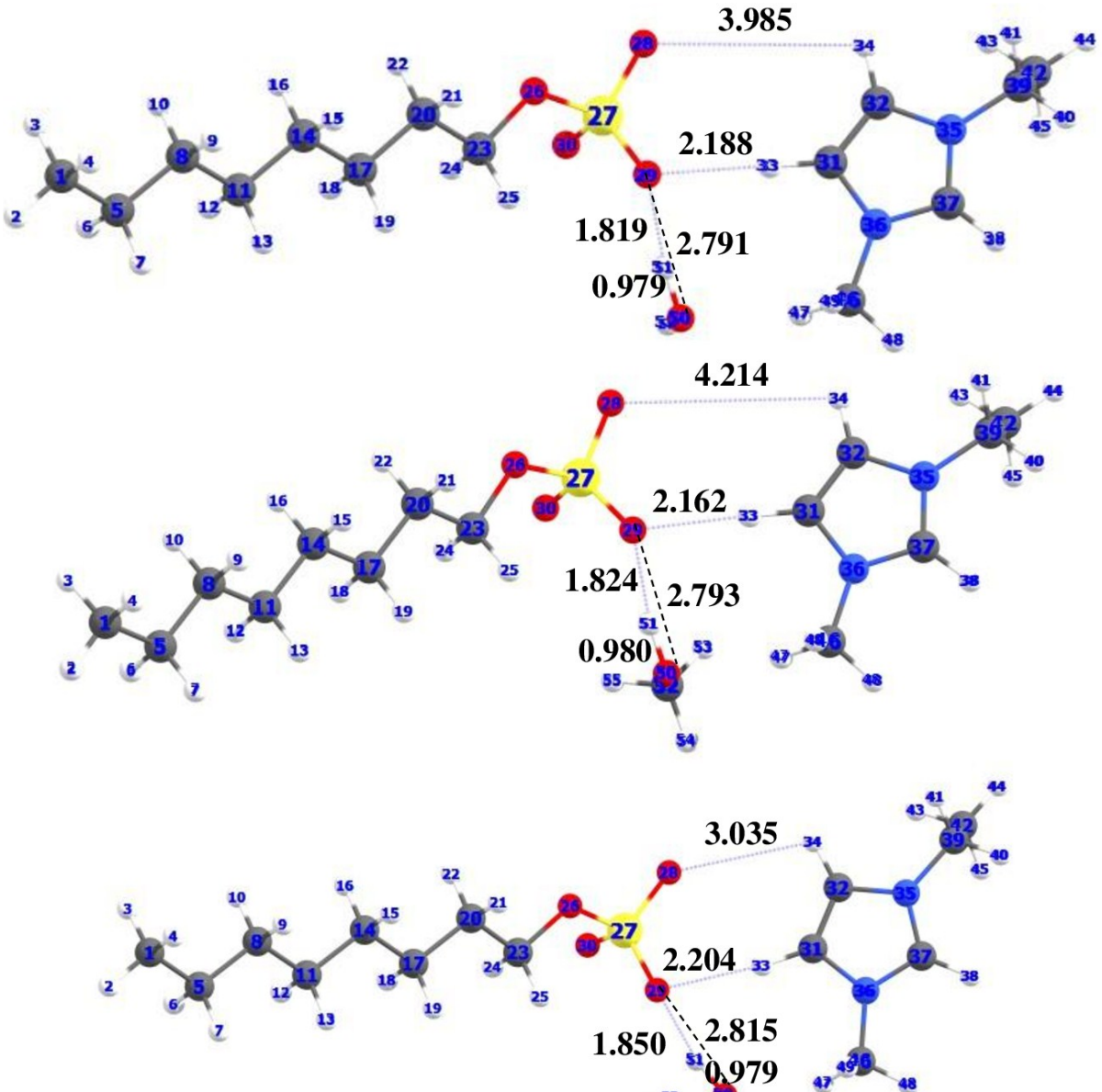

Fig. S14b: Optimized geometries of the [EmimOs], [EmimOs]-Water, [EmimOs]-MeOH, [EmimOs]-iPrOH complexes, calculated at the B3LYP/6-31++G(d,p) level in the solution phase. Bond distances are given in Angstrom unit.